Metabolic Brain Disease (2024) 39:509–522
https://doi.org/10.1007/s11011-023-01339-8

ORIGINAL ARTICLE

Hesperidin counteracts chlorpyrifos-induced neurotoxicity by regulating oxidative stress, inflammation, and apoptosis in rats

Sefa Küçükler[1] · Cuneyt Caglayan[2] · Selçuk Özdemir[3] · Selim Çomaklı[4] · Fatih Mehmet Kandemir[5]

Received: 13 November 2023 / Accepted: 14 December 2023 / Published online: 18 December 2023

Abstract

Chlorpyrifos (CPF), considered one of the most potent organophosphates, causes a variety of human disorders including neurotoxicity. The current study was designed to evaluate the efficacy of hesperidin (HSP) in ameliorating CPF-induced neurotoxicity in rats. In the study, rats were treated with HSP (orally, 50 and 100 mg/kg) 30 min after giving CPF (orally, 6.75 mg/kg) for 28 consecutive days. Molecular, biochemical, and histological methods were used to investigate cholinergic enzymes, oxidative stress, inflammation, and apoptosis in the brain tissue. CPF intoxication resulted in inhibition of acetylcholinesterase (AChE) and butrylcholinesterase (BChE) enzymes, reduced antioxidant status [superoxide dismutase (SOD), catalase (CAT), glutathione peroxidase (GPx) and glutathione (GSH)], and elevation of malondialdehyde (MDA) levels and carbonic anhydrase (CA) activities. CPF increased histopathological changes and immunohistochemical expressions of 8-OHdG in brain tissue. CPF also increased levels of glial fibrillary acidic protein (GFAP) and nuclear factor kappa B (NF-κB) while decreased levels of nuclear factor erythroid 2-related factor 2 (Nrf-2), heme oxygenase-1 (HO-1) and peroxisome proliferator–activated receptor gamma coactivator-1 alpha (PGC-1α). Furthermore, CPF increased mRNA transcript levels of caspase-3, Bax, PARP-1, and VEGF, which are associated with apoptosis and endothelial damage in rat brain tissues. HSP treatment was found to protect brain tissue by reducing CPF-induced neurotoxicity. Overall, this study supports that HSP can be used to reduce CPF-induced neurotoxicity.

Keywords Apoptosis · Chlorpyrifos · Hesperidin · Neurotoxicity, oxidative stress

Introduction

Due to the increasing world population, it is estimated that the food demand will increase by approximately 100% in the next 30 years. Weeds, insect pests, and diseases that hinder agricultural production account for approximately 40% of annual losses. To prevent these agricultural losses and increase production, approximately 2 million metric tons of pesticides are used worldwide each year (Ozturk Kurt and Ozdemir 2023). Globally, environmental pollution is increasing as a result of widespread use of pesticides and the toxicities of pesticides have attracted the attention of people around the world (Caglayan et al. 2019c, 2020; Koksal et al. 2018). Among them, chlorpyrifos (CPF) is a lipophilic, broad-spectrum organophosphate insecticide widely used in agriculture and household applications (Ghahremani et al. 2018; Mahmoud et al. 2019). Humans are mainly exposed to chlorpyrifos through food, water, soil, and air (Kaur et al. 2019; Topal et al. 2014). In some experimental studies, it has been reported that chlorpyrifos causes various neurological, reproductive, respiratory, digestive and circulatory disorders (Kaur et al. 2019; Khalaf et al. 2022; Uzun and Kalender 2013; Yazdinezhad et al. 2017). Because of the lipophilic character of CPF, the nervous system is the main target for CPF; therefore, it can easily cross the blood-brain barrier, causing disruption of neuronal transmission

✉ Cuneyt Caglayan
cuneyt.caglayan@bilecik.edu.tr

1 Department of Biochemistry, Faculty of Veterinary Medicine, Atatürk University, Erzurum, Turkey

2 Department of Medical Biochemistry, Faculty of Medicine, Bilecik Şeyh Edebali University, Bilecik, Turkey

3 Department of Genetics, Faculty of Veterinary Medicine, Atatürk University, Erzurum, Turkey

4 Department of Pathology, Faculty of Veterinary Medicine, Atatürk University, Erzurum, Turkey

5 Department of Medical Biochemistry, Faculty of Medicine, Aksaray University, Aksaray, Turkey

and the development of neurological disorders (Aboubakr et al. 2021). CPF inhibits the acetylcholine esterase (AChE) enzyme, resulting in the accumulation of acetylcholine (ACh) at cholinergic brain synapses and neuromuscular junctions. Accumulation of ACh at cholinergic synapses causes hyperactivity in cholinergic pathways, leading to neurotoxicity and death (Singh and Panwar 2014). In addition, a growing body of research suggests that reactive oxygen species (ROS) induced by CPF are thought to be another mechanism involved in neurotoxicity. Oxidative stress resulting from ROS is known to cause cell damage by damaging cellular biomolecules including proteins, lipids, membranes, and DNA (Aboubakr et al. 2021; Ghahremani et al. 2018; Ozturk Kurt and Ozdemir 2023). CPF has also been reported to increase inflammatory responses by upregulating proinflammatory cytokines such as tumor necrosis factor-α (TNF-α) and interleukin-1β (IL-1β) (El-Sayed et al. 2018).

Hesperidin (HSP) is a pharmacologically active bioflavonoid found in citrus fruits such as oranges and lemons (Caglayan et al. 2019a; Ekinci Akdemir et al. 2016). It has been reported to have pharmacological and biological properties, including, antioxidant (Varışlı et al. 2022), anti-inflammatory (Küçükler et al. 2021), anti-depressive, anti-hypertensive, anti-diabetic (Kandemir et al. 2018), antimicrobial, immunomodulatory (Abuelsaad et al. 2013), hepatoprotective, and nephroprotective (Caglayan et al. 2021). Due to its lipophilic nature and aromatic hydroxyl group, it has been reported that HSP easily crosses the blood-brain barrier and thus is beneficial in the treatment of neurodegenerative diseases (Wang et al. 2021).

This study was designed to further investigate the potential effect of HSP on biochemical, molecular, and histopathological changes in CPF-induced neurotoxicity.

Materials and methods

Chemicals

HSP, CPF and other chemicals are of analytical grade and purchased from Sigma-Aldrich Chemical Company (St. Louis, MO, USA).

Experimental animals

In our study, 35 male Sprague Dawley rats weighing between 250 and 300 g and aged 10–11 weeks were used, which were bred at the Experimental Research and Application Center (ATADEM) of Ataturk University. The animals were kept in cages in a controlled room with a constant temperature of 24–25 °C and a 12-hour light-dark cycle. They had unlimited access to water and standard feed. After one week of acclimatization in their cages, the rats were used for the experiment. The study was conducted in accordance with ethical principles and was approved by the Ataturk University Local Ethics Committee for Animal Experiments (2019/4–77).

Experimental design

CPF was dissolved in corn oil and orally given to rats for 28 days. The rats were randomly divided into five groups of seven rats each.

Group I (Control): Corn oil was given orally for 28 days.

Group II (HSP): Rats were orally treated with HSP (100 mg/kg) daily for 28 days by a gavage.

Group III (CPF): Rats were orally given CPF (6.75 mg/kg) daily for 28 days by a gavage.

Group IV (CPF + HSP-50): 6.75 mg/kg of CPF was administered orally followed by 50 mg/kg/day of HSP given orally 30 min later.

Group V (CPF + HSP-100): 6.75 mg/kg of CPF was administered orally followed by 100 mg/kg/day of HSP given orally 30 min later, both treatments lasting for 28 days.

One day after the last CPF and HSP administration (day 29), the rats were decapitated under sevoflurane anesthesia and their brain tissues were removed. One part of the brain tissues taken was stored at -80 °C for biochemical and molecular analysis, and the other part was taken into 10% buffered formalin solution for histopathological and immunohistochemical analysis.

Determination of CA, AChE and BChE enzyme activities

As described in our previous study (Çelik et al. 2020b), carbonic anhydrase (CA) enzyme activity in brain homogenate was determined using the spectrophotometric method of Verpoorte et al. (1967. AChE and butyrylcholinesterase (BChE) enzyme activities in brain homogenate were studied as described by Ellman et al. (1961 as described our previous study (Çelik et al. 2020b). These enzyme activities were measured spectrophotometrically (UV-1800 Shimadzu, Kyoto, Japan).

Determination of biomarkers of oxidative stress and lipid peroxidation

Brain tissue homogenates required for oxidative stress biomarkers and lipid peroxidation assays were obtained as described in our previous study (Çelik et al. 2020a). The obtained supernatants were used to determine the activities

of superoxide dismutase (SOD), catalase (CAT) and glutathione peroxidase (GPx), and levels glutathione (GSH) and malondialdehyde (MDA). The SOD, CAT and GPx enzyme activities were assayed according to the methods prescribed by (Sun et al. 1988), (Aebi 1984) and (Lawrence and Burk 1976), respectively. GSH level was determined by the method of (Sedlak and Lindsay 1968). Level of MDA was measured following the procedure developed by (Placer et al. 1966). Protein concentration in the brain homogenate was determined using method of (Lowry et al. 1951).

Determination of ELISA markers

In this part, brain tissues ground with liquid nitrogen were homogenized (1/20 w/v) in cold sodium phosphate buffer (0.1 M, pH 7.4) and then centrifuged at 3500 rpm for 20 min to obtain tissue lysates. The supernatants obtained after centrifugation were immediately used in ELISA experiments. Glial fibrillary acidic protein (GFAP), nuclear factor kappa B (NF-κB), nuclear factor erythroid 2-related factor 2 (Nrf2), heme oxygenase-1 (HO-1) and peroxisome proliferator–activated receptor gamma coactivator-1 alpha (PGC-1a) levels in brain tissue were analysed by rat ELISA kits according to the manufacturer's procedure (YL Biont, Shanghai, China). The absorbance was measured at 450 nm.

Quantitative real-time RT-PCR (RT-qPCR)

The total RNA in rat brain tissue was extracted using QIAzol Lysis Reagent (QIAGEN, USA) and RNA was reverse-transcribed into cDNA using QuantiTect Reverse Transcription Kit (Qiagen, Cat: 330,411 Hilden, Germany). The mRNA transcript levels of Caspase 3, Bax, Bcl-2, PARP-1, and VEGF in the brain tissues were examined on a ROTOR-GENE Q 5plex HRM Real-Time PCR Detection System (Qiagen, Hilden, Germany) using QuaniTect SYBR Green PCR Master Mix (Qiagen, Cat: 330,500, Hilden, Germany), which contained a volume of 25 µL. All primer sequences and reaction conditions are shown in Table 1. The $2^{-\Delta\Delta Ct}$ method was used to normalize target gene transcription to GAPDH expression (internal control) to calculate fold induction of target mRNA (Livak and Schmittgen 2001).

Western blot analysis

Total protein was extracted from brain tissues using RIPA lysis buffer with protein inhibitors. The BCA protein assay kit was used to measure the protein concentration. The process of separating proteins was carried out through SDS-PAGE and then transferred onto nitrocellulose membranes which block with 5% bovine serum albumin (BSA). Membranes were incubated overnight with primary antibodies [(PARP (1:1000 dilution, Rabbit Polyclonal, ab227244, Abcam), VEGF (1:1000 dilution, Rabbit Polyclonal, ab46154, Abcam), GAPDH (1:2000 dilution, Rabbit Polyclonal, ab9485, Abcam)]. Following primary antibody incubation, membranes were incubated with the secondary antibody (goat anti-rabbit IgG-HRP 1:5000 dilution, ab6721, Abcam) at room temperature for 2 h. Membranes were exposed and fixed in a dark environment after being submerged in ECL solution for 1 min. Quantification of Western blot images was performed with ChemiDoc™ MP Imaging System (Bio-Rad, California, USA).

Histopathological examination

To determine the histopathological changes, the brain tissues of rats were removed and fixed in a 10% buffered formalin solution for 24 h. After 24 h, the fixation solution was removed by washing the tissues with running tap water. Then, the tissues were dehydrated in a graded series of alcohol solutions (70%, 80%, 96%, and 100% alcohol). The dehydrated tissues were embedded in paraffin after being made clearing with xylene. Thin sections (5 µm) were taken from brain tissues onto normal and polylysine-coated slides using a microtome (Leica, RM2255). The sections were deparaffinized and stained with Hematoxylin & Eosin (H&E). The histopathological changes in the tissues were photographed using a light microscope (Zeiss, Scope A1). Pathological changes occurring in the brain cortex and

Table 1 Primer sequences of Caspase-3, Bax, Bcl2, PARP1, VEGF, and GAPDH

Gene	Sequences (5′-3′)	Length (bp)	Accession no
Caspase-3	F: GGAGCTTGGAACGCGAAGAA R: ACACAAGCCCATTTCAGGGT	169	NM_012922.2
Bax	F: ACACCTGAGCTGACCTTGGA R: AGTTCATCGCCAATTCGCCT	115	NM_016993.1
Bcl-2	F: CTGGTGGACAACATCGCTCT R: GCATGCTGGGGCCATATAGT	115	NM_016993.1
PARP1	F: AAGGCGGAGAAGACATTGGG R: CGCATCTGGCCCTTCTCTAT	101	NM_007415.3
VEGF	F: AACTTCTGGGCTCTTCTCGC R: CTGGGACCACTTGGCATGGT	443	NM_001317041.1
GAPDH	F: AGTGCCAGCCTCGTCTCATA R: GATGGTGATGGGTTTCCCGT	248	NM_017008.4

Table 2 Distribution of lesions in brain tissue according to groups

Lesions	Control	HSP	CPF	CPF + HSP50	CPF + HSP100
Cerebral cortex					
Hyperemia	-	-	+++	+	+
Bleeding	-	-	+++	+	+
Cellular infiltration in the meninges	-	-	++	+	+
Necrosis	-	-	+++	++	+
Neuronal degeneration	-	-	++	+	+
Hippocampus CA2					
Necrosis	-	-	+++	++	+

- No lesion; + mild lesion; ++ moderate lesion; +++ severe lesion

Table 3 Effect of HPS treatment on activities of AChE, BChE and CA enzymes, MDA levels and antioxidant system in CPF-induced brain toxicity in rats

Values are expressed as mean ± SE of seven rats in each group. Statistical significance (*p<0.05, **$p < 0$ 0.01 and ***$p < 0.001$) was analyzed using a One Way ANOVA.

Parameter	Control	HSP	CPF	CPF + HSP50	CPF + HSP100
AChE (U/mg protein)	1.54 ± 0.009	1.62 ± 0.030	1.31 ± 0.012*	1.50 ± 0.014**	1.49 ± 0.12**
BChE (u/mg protein)	0.26 ± 0.002	0.27 ± 0.001	0.21 ± 0.001*	0.26 ± 0.001**	0.25 ± 0.001**
CA (U/mg protein)	3.57 ± 0.07	4.39 ± 0.03**	4.92 ± 0.04*	4.70 ± 0.03**	3.86 ± 0.03**
MDA (nmol/g tissue)	26,67 ± 0,53	26,51 ± 0,63	45,57 ± 0,94*	37,83 ± 0,64**	31,15 ± 0,80***
GSH (nmol/g tissue)	2,58 ± 0,05	2,62 ± 0.04	1,47 ± 0,03*	1,8 ± 0,03**	2,04 ± 0,03***
SOD (U/g protein)	18,11 ± 0,50	18,3 ± 0,68	8,4 ± 0,27*	11,32 ± 0,36**	14,4 ± 0,31***
CAT (Katal/g protein)	13,93 ± 0,4	14,28 ± 0,45	6,05 ± 0,38*	7,28 ± 0,59*	11,54 ± 0,38**
GPx (nmol/g tissue)	19,26 ± 0,50	20,02 ± 0,51	10,88 ± 0,40*	13,79 ± 0,34**	16,99 ± 0,39***

hippocampus CA2 region were evaluated according to the criteria given in Table 2.

Immunohistochemical analysis

For immunohistochemical examination, sections were taken on polylysine-coated slides and then deparaffinized. Endogenous peroxidase activity was quenched by exposing the sections to 3% H_2O_2 and then subjected to antigen retrieval by immersing them in sodium citrate solution (pH 6.0) in a microwave oven at medium power, followed by slow cooling for 20 min. A protein block solution was applied for 10 min to prevent nonspecific binding. Then, the sections were incubated with primary antibody, 8-OHdG (Santa Cruz Biotechnology, Catalog No: sc-66,036, Dilution ratio: 1/200) at room temperature for 1 h. The sections were rinsed with PBS and a biotinylated secondary antibody was applied and incubated for 10 min. After this step, streptavidin-enzyme conjugate binding to biotin on the secondary antibody was applied to the sections and incubated for 15 min. Diaminobenzidine (DAB) chromagen was applied to the tissue sections for 5 min and then washed with PBS. Finally, the sections were counterstained with hematoxylin for 2 min. The immunopositivity of 8-OHdG was scored as follows: absent (-), mild (+), moderate (++), and intense (+++).

Statistical analysis

The statistical analysis was conducted using an automated software (Graph pad prism software Inc., Version 7.0, California, USA). Values are given as means ± S.E for seven rats in each group. Data were analyzed by one-way analysis of variance followed by Tukey's test. Statistically differences were considered to be significant at $p < 0.05$, $p < 0.01$ and $p < 0.001$. The statistical analysis of the immunohistochemical data was performed using the Kruskal-Wallis test followed by the Mann-Whitney U test. Values are given as means ± S.E for seven rats in each group. Statistically differences were considered to be significant at $p < 0.05$.

Results

Effect of HSP on CA, AChE and BChE activities in CPF-induced brain toxicity

In this study, AChE and BChE enzyme activities were decreased while CA enzyme activities were significantly ($p < 0.05$) increased in the CPF group compared to the control group. Treatment of HSP (50 and 100 mg/kg) increased AChE and BChE activities and decreased CA activities ($p < 0.01$, Table 3).

Effect of HSP on antioxidant enzymes and lipid peroxidation in CPF-induced brain toxicity

In the present study, we found that CPF exposure induced a significant decrease ($p < 0.05$) in crucial antioxidant biomarkers (SOD, CAT, GPx and GSH) that play a major role in preventing free radical toxicity. Co-administration of HSP (50 and 100 mg/kg) was found to significantly ($p < 0.001$) increase these antioxidant biomarkers (Table 3). In addition, MDA, a marker of lipid peroxidation, was found to increase with CPF application. However, the CPF-induced increase in MDA level was significantly attenuated after treatment with HSP ($p < 0.001$).

Effect of HSP on GFAP, NF-κB, Nrf2, HO-1 and PGC-1a levels in CPF-induced brain toxicity

When compared to the control group, it was an increase in GFAP and NF-κB levels in the CPF group while a decrease in Nrf2, HO-1 and PGC-1a levels ($p < 0.05$). Compared to the CPF group, the CPF + HSP-50 and CPF + HSP-100 groups showed a decrease in GFAP and NF-κB levels and a dose-dependent increase in Nrf2, HO-1, and PGC-1a levels ($p < 0.001$, Fig. 1A-E).

Effect of HSP on Caspase-3, Bax, Bcl-2, PARP-1, VEGF, and GAPDH levels in CPF-induced brain toxicity

The mRNA transcript levels of caspase-3, Bax, Bcl-2, PARP-1, and VEGF were measured using qRT-PCR. The expression of caspase-3, Bax, PARP-1, and VEGF in brain tissues was found to be similar levels in the control and HSP groups. However, the expression levels of these genes increased in the CPF group ($p < 0.01$). In the CPF + HSP-50 and CPF + HSP-100 groups, the expression levels decreased compared to the CPF alone group. The expression level of Bcl-2 decreased in the CPF group, while it increased in the CPF + HSP-50 and CPF + HSP-100 groups ($p < 0.05$, Fig. 2A-E).

Effect of HSP on PARP-1 and VEGF protein levels in CPF-induced brain toxicity

The levels of PARP-1 and VEGF proteins were determined in rat brain tissues. The expression levels of these proteins

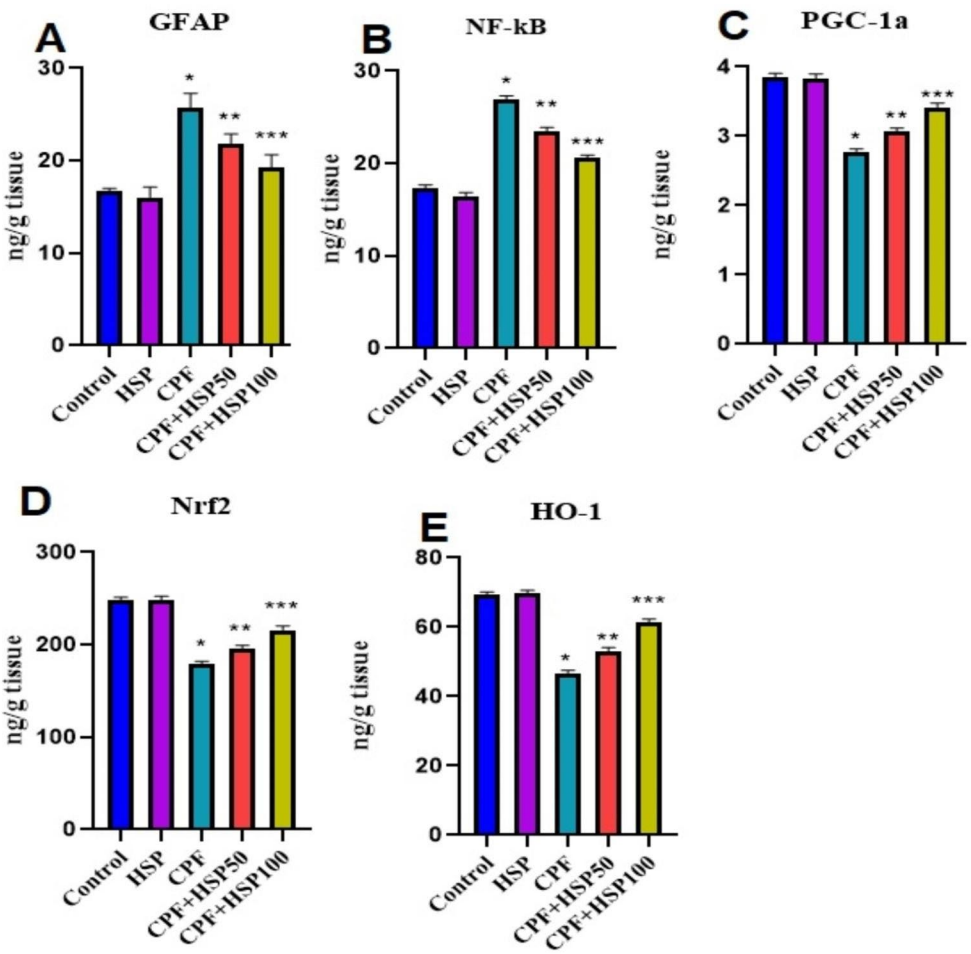

Fig. 1 Effect of HPS treatment on GFAP, NF-κB, Nrf2, HO-1 and PGC-1a levels in CPF-induced brain toxicity in rats. Data are expressed as the mean ± SE. *$P < 0.05$, **$P < 0.01$ and ***$P < 0.001$ vs. model group

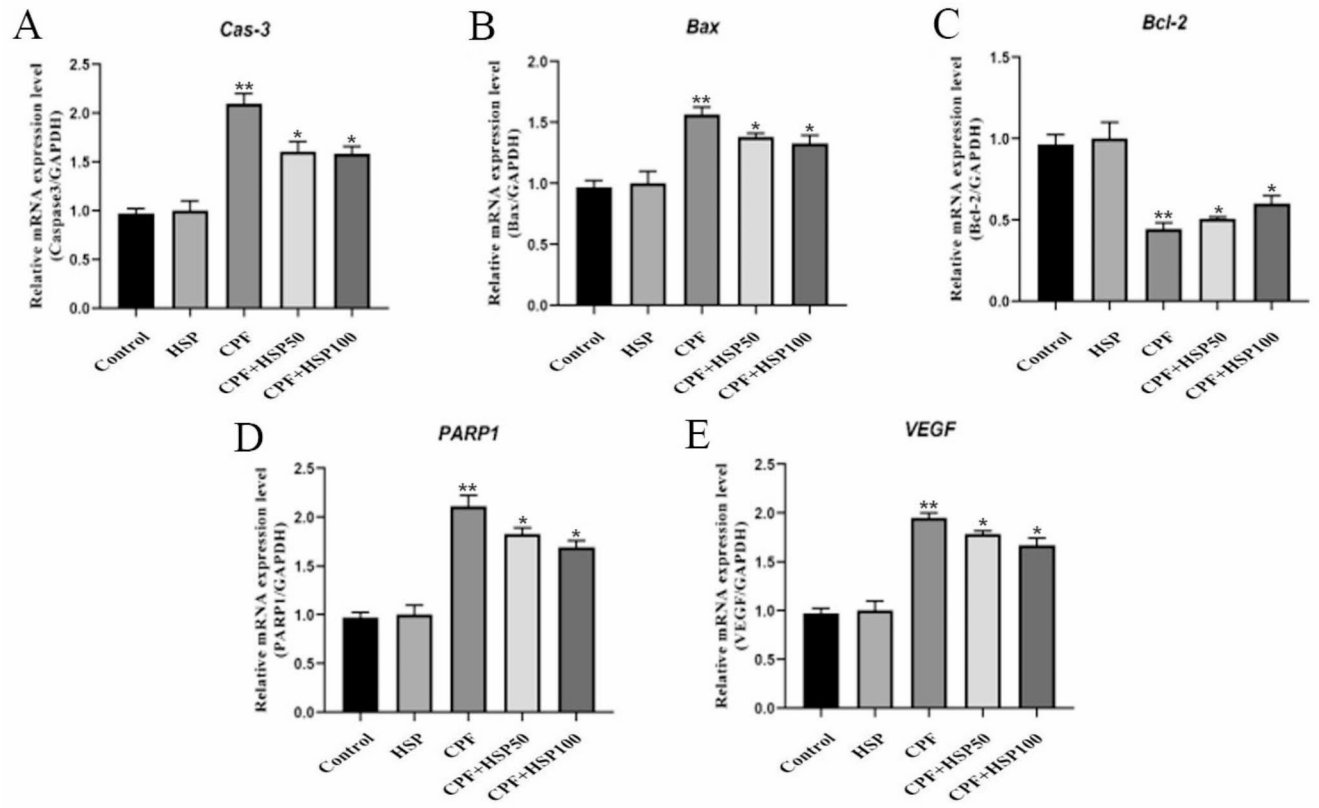

Fig. 2 Effects of HSP on the mRNA expression of caspase-3, Bax, Bcl-2, PARP-1, and VEGF in CPF-indeced brain toxicty (**A**-**E**). The mRNA expression of these genes was detected by RT-PCR and datas were generated from brain tissue. Data are expressed as the mean ± SE. $^{*}P < 0.05$, $^{**}P < 0.01$ vs. model group

were found to be the same in the control and HSP groups ($p > 0.05$). While the levels of these proteins increased in the CPF group, they decreased in the CPF + HSP-50 and CPF + HSP-100 groups compared to the CPF alone group ($p < 0.05$; Fig. 3).

Histopathological results

In the histopathological examination of the cortical region of the brain, the molecular layer showed normal cellular structure in the control and HSP-treated rats (Fig. 4A and B). Rats treated with CPF exhibited degeneration in neurons, an increase in hyperchromatic nuclei, and necrotic structures containing pyknotic changes in the nuclei. The meningeal vessels were extremely hyperemic, with mononuclear cell infiltrations present (Fig. 4C). In the group where CPF was administered with HSP at a dose of 50 mg/kg, a decrease in the number of degenerative and necrotic neurons and the hyperemic findings in the meninges compared to the group treated with only CPF was observed (Fig. 4D). In the group where CPF was administered with HSP at a dose of 100 mg/kg, the hyperemia in the meninges continued, but a significant decrease in the number of necrotic neurons was observed (Fig. 4E).

In the hippocampal CA2 region of the brain, normal histological appearance was observed in the control and HSP-treated rats (Fig. 5A and B). Degenerated and vacuolated neurons with changes in the form of shrunken, pyknotic, and hyperchromatic nuclei were observed in rats treated with CPF (Fig. 5C). In the group treated with CPF plus 50 mg/kg HSP, a decrease in the number of neurons with pyknotic and hyperchromatic nuclei was observed (Fig. 5D). Particularly in the group treated with CPF plus 100 mg/kg HSP, the number of necrotic cells decreased and was similar to the control and HSP groups (Fig. 5E).

Immunohistochemical staining for 8-OHdG

Immunohistochemical staining was used to evaluate the formation of 8-OHdG, a marker of oxidative DNA damage. No 8-OHdG positivity was detected in the control and only HSP-treated groups (Fig. 6A and B). In the cortex region of the brain, a strong 8-OHdG expression was observed in the cytoplasm of neurons in the group treated with CPF (Fig. 6C). In the group treated with CPF + HSP 50 mg/kg, it was determined that this expression level was significantly reduced compared to the CPF group (Fig. 6D), this difference was not significant. The expression levels were very low in

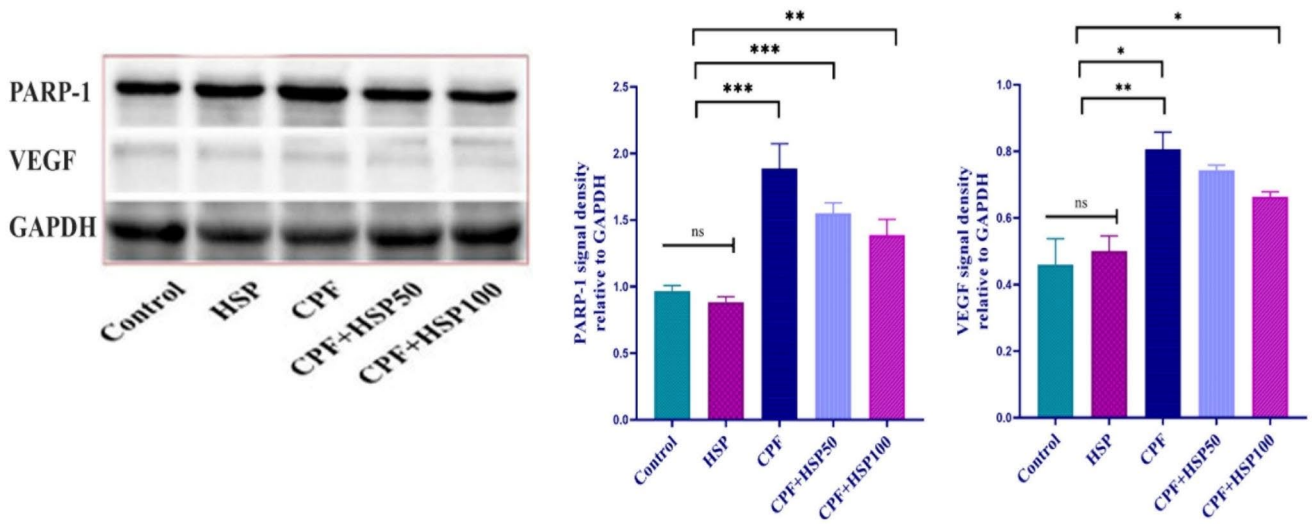

Fig. 3 Expression levels of PARP-1 and VEGF proteins. Protein levels of PARP-1 and VEGF in brain tissue. Data are expressed as the mean ± SE. $^{*}P < 0.05$, $^{**}P < 0.01$ and $^{***}P < 0.001$ vs. model group

the group treated with CPF + HSP 100 mg/kg compared to the CPF and CPF + HSP 50 mg/kg groups (Fig. 6E). In the hippocampal CA2 region of the brain, very mild 8-OHdG positivity was detected in the control and only HSP-treated groups (Fig. 7A and B). In the hippocampal CA2 region of the brain, where neurons were stained with 8-OHdG, a significant increase in expression level was observed in rats treated with CPF and CPF + HSP 50 mg/kg (Fig. 7C and D). In the group treated with CPF + HSP 100 mg/kg, the immunopositivity of 8-OHdG was significantly reduced compared to the group treated with CPF alone (Fig. 7E).

Discussion

CPF is a well-known organophosphate insecticide that was commonly used in agricultural purposes to control pests on several crops, including as fruits, vegetables, and grains. It belongs to a class of chemicals known as organophosphates, which are derived from phosphoric acid (Nandhini et al. 2021). It acts by inhibiting the activity of an enzyme called AChE by phosphorylating the serine OH group of AChE. This causes a buildup of ACh in the brain and overstimulation of the cholinergic nervous system, which results in a number of clinical problems (Landis et al. 2020). AChE is a crucial enzyme for the nervous system and is therefore regarded as a classic biomarker for neurotoxicity caused by organophosphates (Fereidouni et al. 2019). On the other hand, BChE enzyme acts on butyrylcholine by catalyzing the breakdown of neurotransmitters into choline and butyrate and stops their effects in the synaptic cleft (Sulumer et al. 2023). AChE and BChE are inhibited by organophosphate and carbamates, including CPF. The CPF induces irreversible ChE inhibition, triggering constant stimulation of the muscles, leading to paralysis and death (Botté et al. 2012). Research have suggested that exposure to CPF may have adverse effects on the neurological development and brain toxicity (Abd-Elhakim et al. 2023). Along with the aforementioned, the current study confirmed that a marked drop in AChE and BChE levels in CPF-intoxicated rats relative to controls explained CPF-induced neurotoxicity. These results are in line with those from other studies by (AlKahtane et al. 2020; Fereidouni et al. 2019; Mahmoud et al. 2019) which showed that CPF causes neurotoxicity linked to decreased levels of AChE. Similarly to this, lower blood levels of AChE may reflect AChE's decreased activity in the brain following disruption of cholinergic transmission induced by CPF (Albasher et al. 2020). Organophosphates, which are phosphoric acid esters and belong to one of the most popular pesticide families known for their ability to cause neurotoxicity by inhibiting cholinesterase, shown a definite inhibitory capability on CA activity. (Lionetto et al. 2020). It has been demonstrated that a number of substances related to environmental contamination impair CA's catalytic activity. Among these, several studies have shown that CA is sensitive to pesticides in both people and wildlife. Their IC_{50} values ranged from nanomolar to millimolar, displaying a great degree of variation across particular pesticides in the same class, as well as between species and tissues. For instance, the IC_{50} values for dichlorvos, methamidophos, and methylparathion in bovine CA erythrocytes were similar and in the micromolar range, whereas the IC_{50} for CPF was one order of magnitude higher and indicated a decreased sensitivity (Demirdağ et al. 2012). This finding demonstrates that the CA inhibition of particular pesticides belonging to the same class of organophosphates can

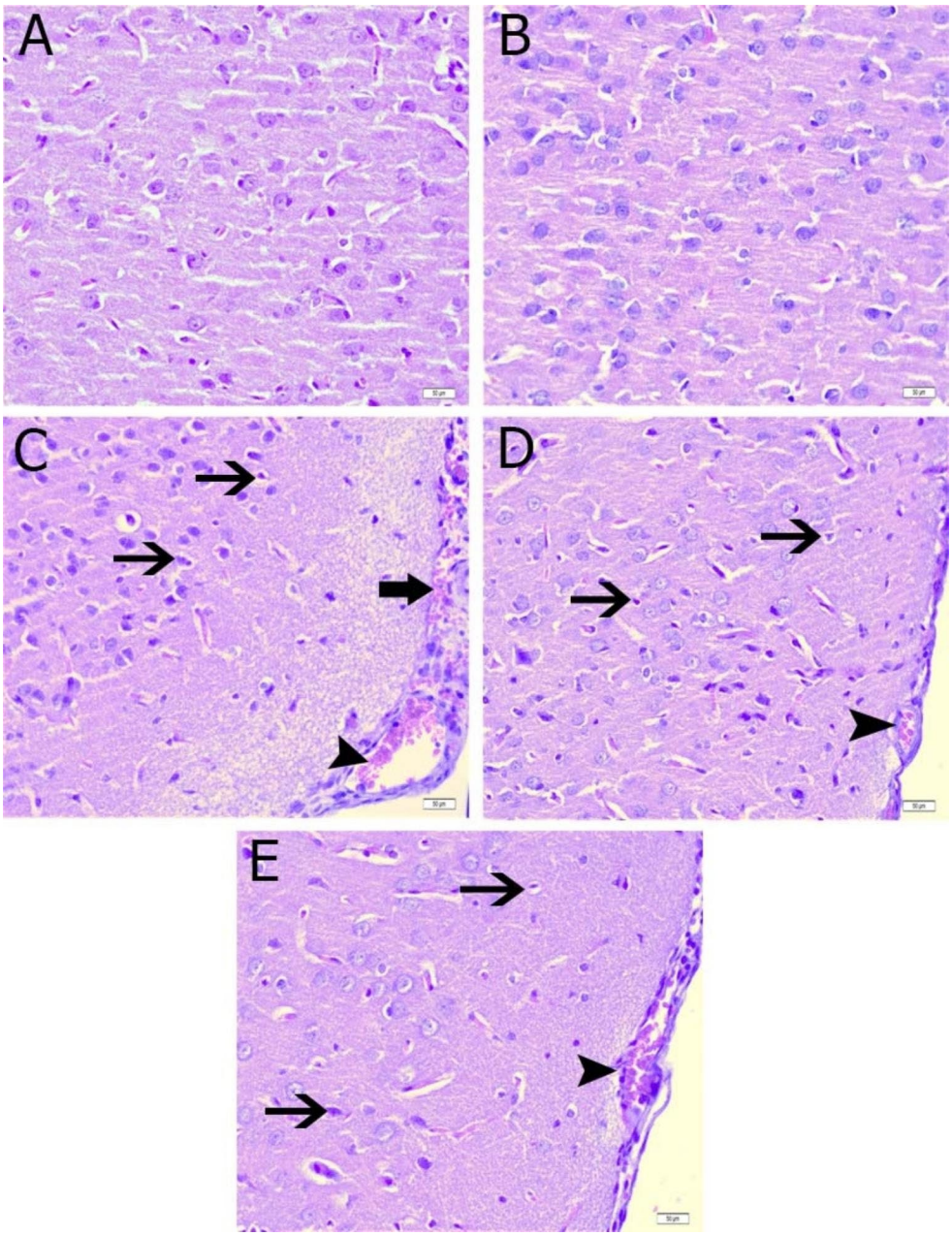

Fig. 4 Paraffin sections were stained with hematoxylin and eosin (H&E) to determine histopathological changes. Brain cortex of control group (**A**) and rats treated with HSP (**B**): neurons with normal histological appearance in the cortex region. Brain cortex section of rats treated with CPF (**C**): severe hyperemia (arrowhead) and areas of bleeding (thick arrow) in meningeal vessels, necrotic neuronal cells with pyknotic and hyperchromatic nuclei (thin arrow). Brain cortex section of rats treated with 50 mg/kg HSP together with CPF (**D**): mild hyperemia (arrowhead) in meningeal vessels, necrotic neuronal cells with moderately pyknotic and hyperchromatic nuclei (thin arrow). Brain cortex section of rats treated with 100 mg/kg HSP together with CPF (**E**): hyperemia (arrowhead) in meningeal vessels, slightly pyknotic and hyperchromatic nucleus neuronal cells (thin arrow). Bar: 50 µm

vary. In the present study, a decrease in AChE and BChE activities and an increase in CA activities were observed in CPF-induced neurotoxicity compared to the control group. HSP administered therapeutically was found to significantly regulate these values in a dose-dependent manner compared to the CPF-induced group.

CPF has been reported to induce oxidative injury via the excess generation of ROS. When the amounts of ROS exceed the scavenging activities of the antioxidant response system, the brain is one of the most susceptible tissue to oxidative damage (Samina 2017). According to our findings, administering CPF led to statistically significant increases in brain LPO levels and decreases in antioxidant activities including SOD, CAT, GPx and GSH. These results are in line with earlier research, which showed that CPF and other pesticides caused oxidative damage, which was supported by an increase in LPO and a decrease in the levels of the antioxidant enzymes SOD, CAT, and GPx (Aboubakr et al. 2021; Ćupić Miladinović et al. 2021; Hassan et al. 2022). These findings are likely due to an excessive formation of ROS, which may be connected to the leakage of brain enzymes. The loss of healthy cells that can respond to oxidative stress and cellular injury was the cause of the decrease in antioxidant enzyme activity in the brain tissue. On the other hand, it might be brought on by the CPF's inability to adequately detoxify substances and damage from ROS.

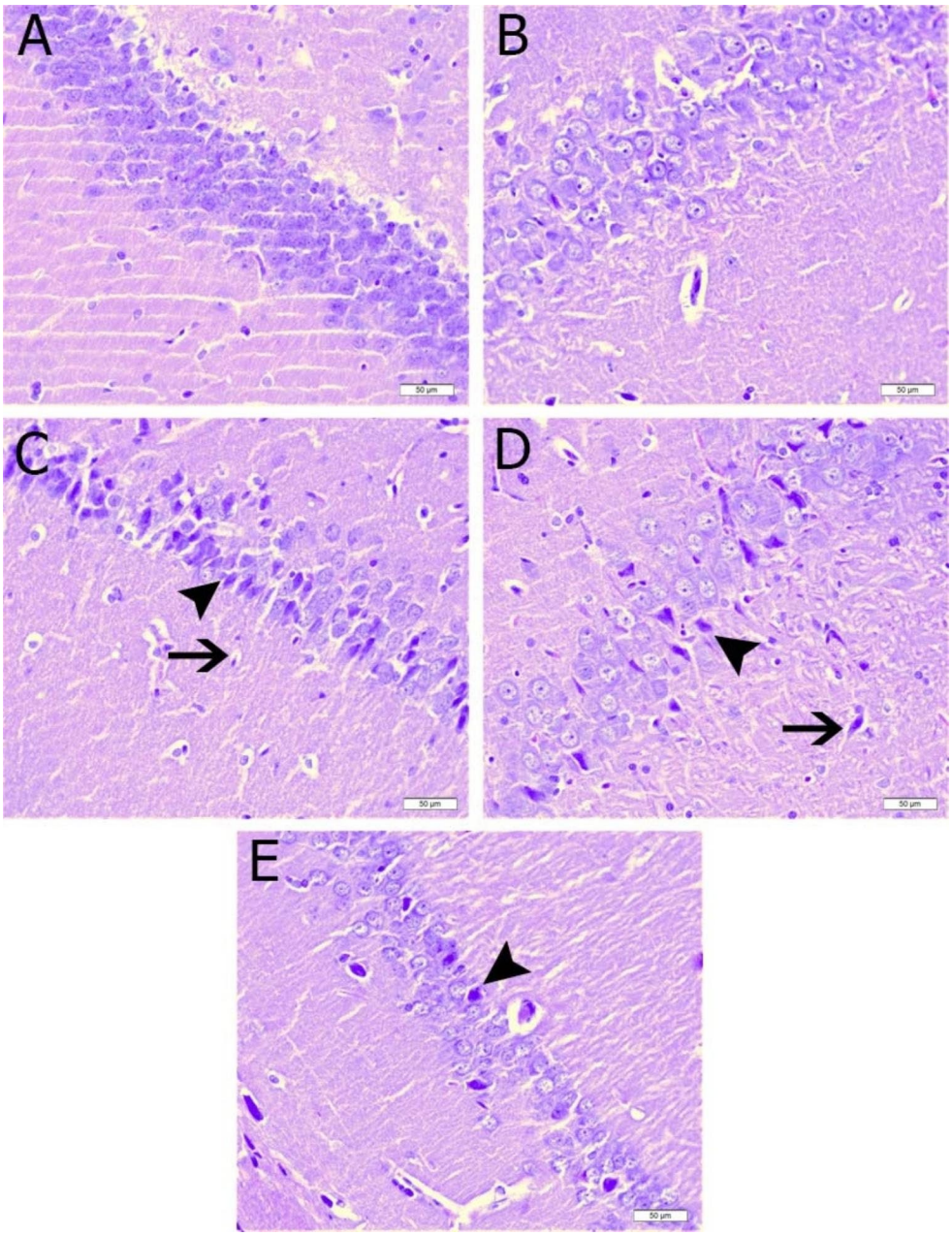

Fig. 5 Paraffin sections were stained with hematoxylin and eosin (H&E) to determine histopathological changes. Hippocampal region of control group (**A**) and rats treated with HSP (**B**): normal histological appearance of neurons in the pyramidal cell layer of CA2 region. Hippocampal region of rats treated with CPF (**C**): severe shrunken and necrotic hyperchromatic neuronal cells (arrowhead) in the pyramidal cell layer of CA2 region. Hippocampal region of rats treated with CPF and 50 mg/kg HSP (**D**): decreased necrotic neuronal cells (arrowhead) and pyknotic nuclei in the pyramidal cell layer of CA2 region. Hippocampal region of rats treated with CPF and 100 mg/kg HSP (**E**): slightly hyperchromatic necrotic neuronal cells (arrowhead) and mild hyperemia in the blood vessel in the pyramidal cell layer of CA2 region. Scale bar: 50 µm

By scavenging superoxide anions and hydroxyl ions, the antioxidant enzymes SOD, CAT, and GPx activities help to defend against the harmful effects of LPO. HSP is often associated with various health benefits. It is believed to have antioxidant effects, which means it can help protect cells from damage caused by free radicals (Wdowiak et al., 2022). In our study, the administration of HSP against CPF led to an increase in SOD, CAT, and GPx activities in the brain tissues. A preventative course of HSP treatment also restored the MDA level, indicating a reduction in LPO suggesting that HSP could be used to prevent brain damage particularly those induced by oxidative damage.

We assume that Nrf2/HO-1 signaling pathway is engaged in the protective mechanism of HSP given its crucial roles in regulating redox homeostasis and preventing inflammation (Emre Kızıl et al. 2023). An efficient method for boosting antioxidant and anti-inflammatory defenses and safeguarding the cells from the damaging effects of high ROS is activating Nrf2/HO-1 pathway (Kızıl et al. 2023). Intoxication with CPF has been shown to decrease mRNA transcript levels of Nrf2 and HO-1 in our study. CPF treatment has been reported to inhibit Nrf2 signaling in rat liver (Küçükler et al. 2021), human neuroblastoma and glioblastoma cells (Brasil et al. 2021; Hsu et al. 2023). Here, HSP increased HO-1 and Nrf2 in the brain of rats given CPF. This accounted for the

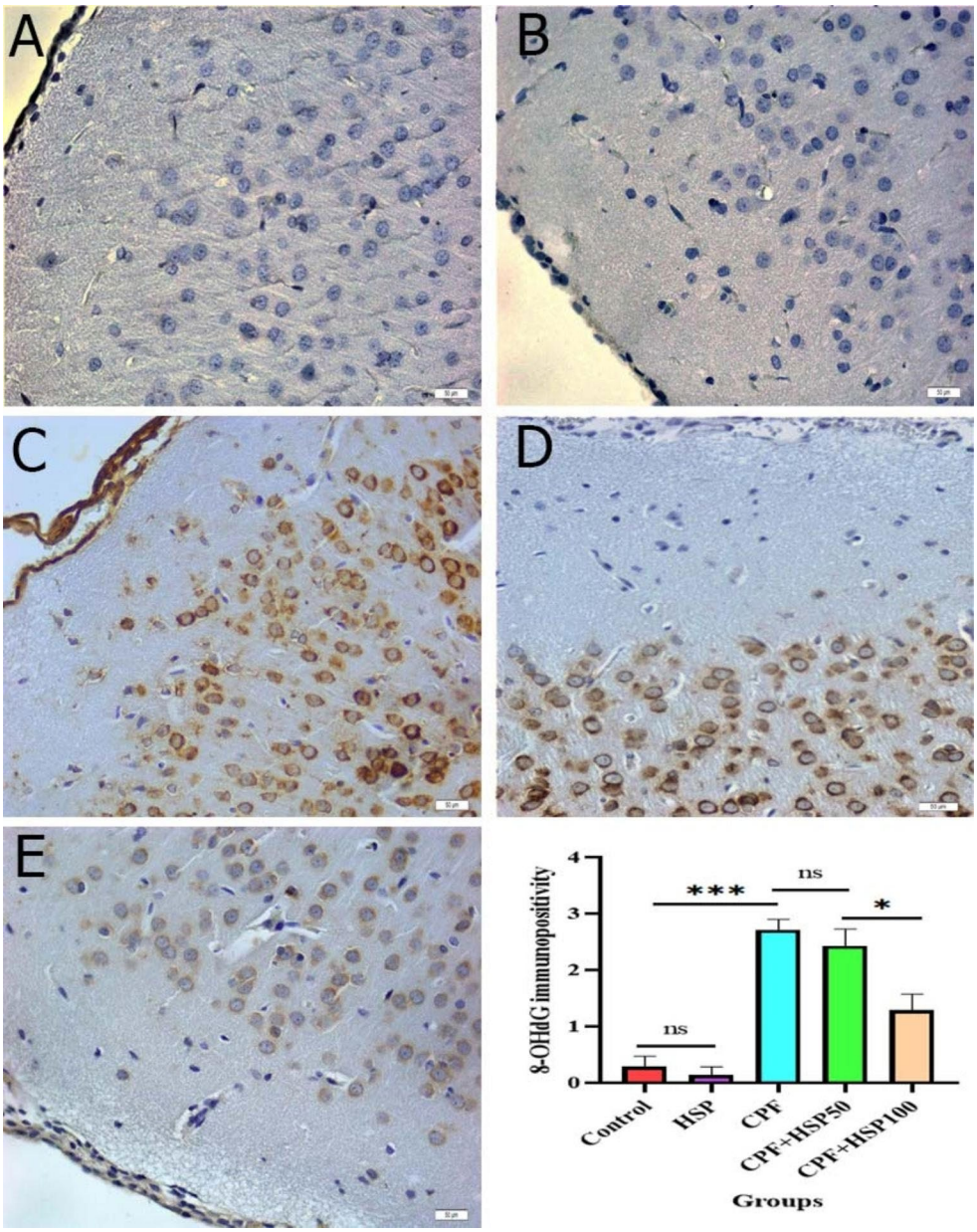

Fig. 6 Immunoreactivity of brain 8-OHdG. Photomicrographs showing the immunoreactivity of 8-OHdG (brown areas) in the cytoplasm of neurons (arrows) in the rat brain cortex from the control group (**A**), HSP group (**B**), CPF group (**C**), CPF + HSP-50 group (**D**), and CPF + HSP-100 group (**E**). Significant increases in 8-OHdG immunoreactivity were observed in rats treated with CPF and CPF + HSP-50, while treatment with CPF + HSP-100 significantly reduced 8-OHdG immunoreactivity at the end of the treatment period (histogram). (n: no significant, $*p < 0.05$, $***p < 0.05$, n = 7)

increased antioxidant enzymes and decreased ROS in the brain of rats exposed to CPF. These results provided confirmation for earlier studies that indicated Nrf2 and HO-1 were involved in the ameliorative effect of HSP against apoptosis and oxidative stress in hepato-renal tissues (Küçükler et al. 2021). In addition to reducing ROS, Nrf2 and HO-1 can reduce inflammation by preventing NF-κB signaling, the inflammatory response, and inflammation by triggering anti-inflammatory mediators (Wardyn et al., 2015). In our in vivo study, it was shown that HSP significantly increased the levels of Nrf2, HO-1 and PGC-1α in CPF-induced brain damage.

Apoptosis is thought to be a critical mechanism of CPF-induced toxicity (Albasher et al. 2019). We looked into the expression levels of Bcl-2, Bax, and caspase-3 in order to further reveal the potential ameliorative effects of HSP for preventing CPF-induced apoptosis in brain tissue. We demonstrated that HSP significantly reduced CPF up-regulated Bax and caspase-3 mRNA expression while down-regulating Bcl-2 mRNA expression. Bcl-2 is a crucial apoptosis regulator, and its overexpression is linked to the inhibition of ROS-induced death. Contrarily, overexpression of Bax and caspase-3 intensifies cellular dysfunction and encourages proapoptotic signaling (Obeng 2020). An earlier study found that exposure to CPF decreased Bcl-2 and increased Bax and caspase-3, indicating that CPF may cause cell death through caspase-dependent mitochondrial mechanisms (Zhang et al. 2018). Apoptotic cascade induction

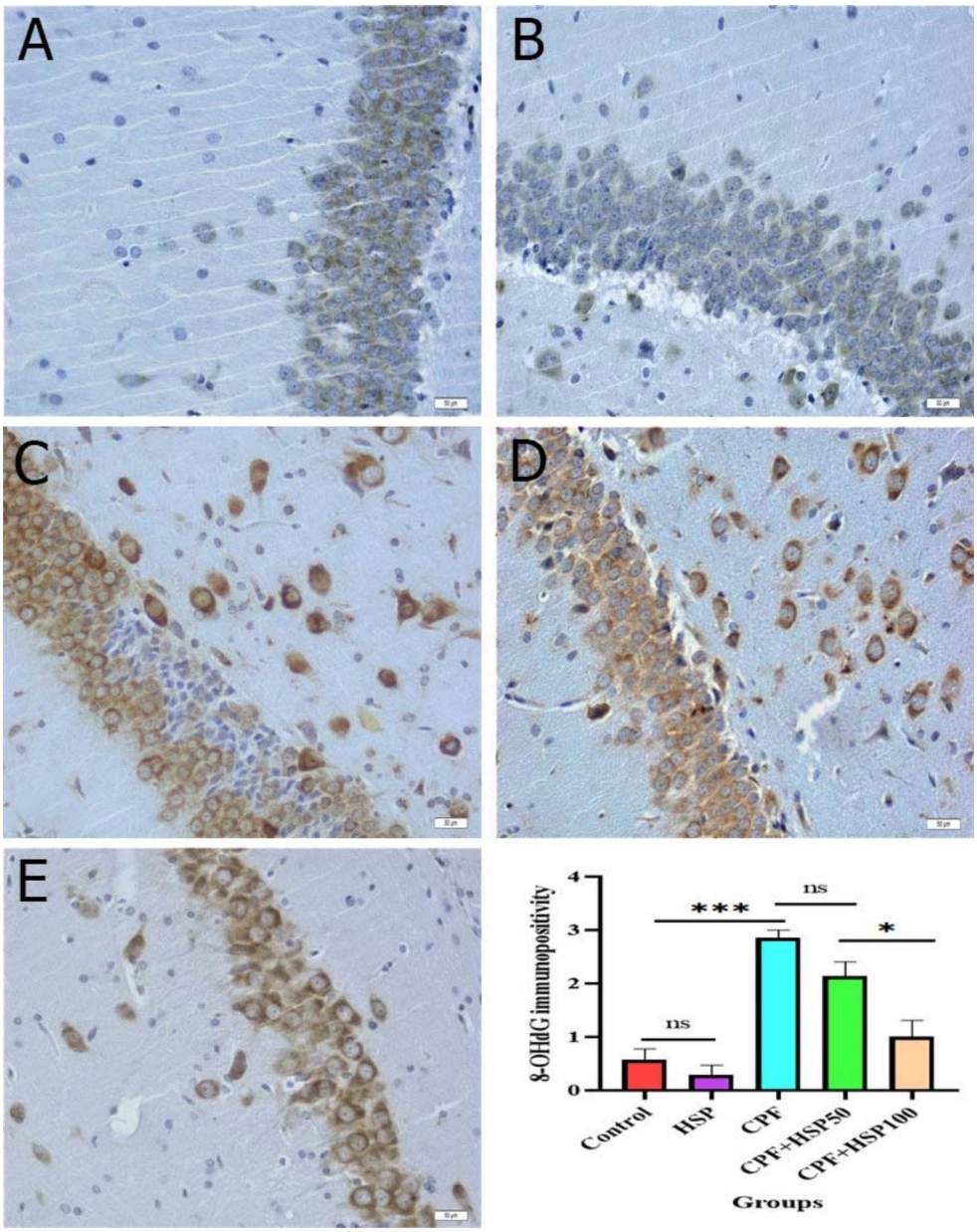

Fig. 7 8-OHdG immunoreactivity in the hippocampus region. Photomicrographs showing 8-OHdG immunoreactivity (brown regions) in the cytoplasm of neurons (arrowheads) in the pyramidal cell layer of the hippocampus region of control group (**A**), HSP group (**B**), CPF group (**C**), CPF + HSP-50 group (**D**), and CPF + HSP-100 group (**E**) rats. The 8-OHdG immunoreactivity significantly increased in rats treated with CPF and CPF + HSP-50, while treatment with CPF + HSP-100 significantly reduced the 8-OHdG immunoreactivity at the end of the treatment period (histogram) (n: no significant, *$p < 0.05$, ***$p < 0.05$, n = 7)

in response to CPF has also been linked to mitochondrial malfunction and excessive ROS generation linked to the development of oxidative stress (Seth et al. 2021). Additionally, it has been demonstrated that CPF induces apoptosis by increasing proapoptotic proteins in liver and renal tissues (Küçükler et al. 2021). In this study, administration of CPF significantly increased Caspase-3 and Bax levels and decreased Bcl-2 levels reflecting apoptotic responses, whereas HSP showed an anti-apoptotic effect by regulation of these markers.

The histopathological investigation demonstrated that CPF causes brain damage as evidenced by the observation of hyperemia, bleeding, cellular infiltration in the meninges, necrosis, and neuronal degeneration in the cortical region and hippocampal CA2 region. Our histopathological results were that HSP treatment contributed to the recovery of CPF-induced brain damage. On the other hand, 8-OHdG is considered a best-documented biomarker of oxidative DNA damage (Caglayan et al. 2019b). Free radicals formed as a result of oxidative stress interact with DNA to produce damages such as double- and single-stranded DNA breaks, nucleoside modifications and deletions. As a result of these interactions, the formation of 8-OHdG is inevitable (Benzer et al. 2018). A previous study reported that CPF caused oxidative DNA damage by increasing the level of 8-OHdG in rat liver and kidney tissues (Owumi et al. 2022). In our study, 8-OHdG expression increased in CPF-induced brain

damage. HSP treatment significantly decreased the expression of 8-OHdG.

Conclusion

The long-term treatment of rats with CPF exhibited remarkable neurotoxic effects, demonstrated by decreased AChE and BChE levels, increased pro-inflammatory cytokines and apoptosis, as well as altered oxidative status. HSP provided protection against CPF-induced neurotoxicity by reducing oxidative stress, inflammation and apoptosis, possibly due to its antioxidant and anti-inflammatory activity.

Author contributions SK and FMK designed the research. SK, CC, SÖ, SÇ and FMK conducted experiments. CC, FMK, and SÇ analyzed data. CC wrote the manuscript. All the authors have read and approved the final version for publication.

Funding This work was supported by Grants from the Scientific Research Projects Coordination Unit of Atatürk University (Project Code: TSA-2019-7303, Project ID: 7303). Therefore, we are grateful to Atatürk University, Turkey.

Data Availability All data generated or analyzed during this study are included in this published article.

Declarations

Conflict of interest The authors have no confict of interest.

Ethical approval Ethics committee approval of the study was obtained from Ataturk University Local Ethics Committee for Animal Experiments (2019/4–77).

Consent to participate Not applicable.

Consent for publication The authors give their consent for the publication of this manuscript.

References

Abd-Elhakim YM, El Sharkawy NI, Gharib HSA, Hassan MA, Metwally MMM, Elbohi KM et al (2023) Neurobehavioral responses and toxic brain reactions of juvenile rats exposed to iprodione and chlorpyrifos, alone and in a mixture. Toxics 11,

Aboubakr M, Elshafae SM, Abdelhiee EY, Fadl SE, Soliman A, Abdelkader A et al (2021) Antioxidant and anti-inflammatory potential of thymoquinone and lycopene mitigate the chlorpyrifos-induced toxic neuropathy. Pharmaceuticals 14,

Abuelsaad ASA, Mohamed I, Allam G, Al-Solumani AA (2013) Antimicrobial and immunomodulating activities of hesperidin and ellagic acid against diarrheic aeromonas hydrophila in a murine model. Life Sci 93:714–722

Aebi H (1984) [13] catalase in vitro. Methods Enzymol 105:121–126

Albasher G, Almeer R, Alarifi S, Alkhtani S, Farhood M, Al-Otibi FO et al (2019) Nephroprotective role of beta vulgaris L. root extract against chlorpyrifos-induced renal injury in rats. Evidence-Based Complement Altern Med 2019:359561

Albasher G, Alsaleh AS, Alkubaisi N, Alfarraj S, Alkahtani S, Farhood M et al (2020) Red beetroot extract abrogates chlorpyrifos-induced cortical damage in rats. Oxid Med Cell Longev. 2963020

AlKahtane AA, Ghanem E, Bungau SG, Alarifi S, Ali D, AlBasher G et al (2020) Carnosic acid alleviates chlorpyrifos-induced oxidative stress and inflammation in mice cerebral and ocular tissues. Environ Sci Pollut Res 27:11663–11670

Benzer F, Kandemir FM, Kucukler S, Comaklı S, Caglayan C (2018) Chemoprotective effects of curcumin on doxorubicin-induced nephrotoxicity in wistar rats: by modulating inflammatory cytokines, apoptosis, oxidative stress and oxidative DNA damage. Arch Physiol Biochem 124:448–457

Botté ES, Jerry DR, Codi King S, Smith-Keune C, Negri AP (2012) Effects of chlorpyrifos on cholinesterase activity and stress markers in the tropical reef fish Acanthochromis polyacanthus. Mar Pollut Bull 65:384–393

Brasil FB, de Almeida FJS, Luckachaki MD, Dall'Oglio EL, de Oliveira MR (2021) Pinocembrin pretreatment counteracts the chlorpyrifos-induced HO-1 downregulation, mitochondrial dysfunction, and inflammation in the SH-SY5Y cells. Metab Brain Dis 36:2377–2391

Caglayan C, Demir Y, Kucukler S, Taslimi P, Kandemir FM, Gulçin İ (2019a) The effects of hesperidin on sodium arsenite-induced different organ toxicity in rats on metabolic enzymes as antidiabetic and anticholinergics potentials: a biochemical approach. J Food Biochem 43:e12720

Caglayan C, Kandemir FM, Yildirim S, Kucukler S, Eser G (2019b) Rutin protects mercuric chloride-induced nephrotoxicity via targeting of aquaporin 1 level, oxidative stress, apoptosis and inflammation in rats. J Trace Elem Med Biol 54:69–78

Caglayan C, Taslimi P, Türk C, Kandemir FM, Demir Y, Gulcin İ (2019c) Purification and characterization of the carbonic anhydrase enzyme from horse mackerel (Trachurus trachurus) muscle and the impact of some metal ions and pesticides on enzyme activity. Comp Biochem Physiol C: Toxicol Pharmacol 226:108605

Caglayan C, Taslimi P, Türk C, Gulcin İ, Kandemir FM, Demir Y et al (2020) Inhibition effects of some pesticides and heavy metals on carbonic anhydrase enzyme activity purified from horse mackerel (Trachurus trachurus) gill tissues. Environ Sci Pollut Res 27:10607–10616

Caglayan C, Kandemir FM, Darendelioğlu E, Küçükler S, Ayna A (2021) Hesperidin protects liver and kidney against sodium fluoride-induced toxicity through anti-apoptotic and anti-autophagic mechanisms. Life Sci 281:119730

Çelik H, Kandemir FM, Caglayan C, Özdemir S, Çomaklı S, Kucukler S et al (2020a) Neuroprotective effect of rutin against colistin-induced oxidative stress, inflammation and apoptosis in rat brain associated with the CREB/BDNF expressions. Mol Biol Rep 47:2023–2034

Çelik H, Kucukler S, Çomaklı S, Özdemir S, Caglayan C, Yardım A et al (2020b) Morin attenuates ifosfamide-induced neurotoxicity in rats via suppression of oxidative stress, neuroinflammation and neuronal apoptosis. Neurotoxicology 76:126–137

Ćupić Miladinović D, Prevendar Crnić A, Peković S, Dacić S, Ivanović S, Santibanez JF et al (2021) Recovery of brain cholinesterases and effect on parameters of oxidative stres and apoptosis in quails (Coturnix japonica) after chlorpyrifos and vitamin B1 administration. Chemico-Biol Interact 333:109312

Demirdağ R, Yerlikaya E, Aksakal E, Küfrevioğlu ÖI, Ekinci D (2012) Influence of pesticides on the pH regulatory enzyme, carbonic anhydrase, from European Seabass liver and bovine erythrocytes. Environ Toxicol Pharmacol 34:218–222

Ekinci Akdemir FN, Gülçin İ, Karagöz B, Soslu R, Alwasel SH (2016) A comparative study on the antioxidant effects of hesperidin and

ellagic acid against skeletal muscle ischemia/reperfusion injury. J Enzyme Inhib Med Chem 31:114–118
El-Sayed NM, Ahmed AAM, Selim MAA (2018) Cytotoxic effect of chlorpyrifos is associated with activation of Nrf-2/HO-1 system and inflammatory response in tongue of male Wistar rats. Environ Sci Pollut Res 25:12072–12082
Ellman GL, Courtney KD, Andres V, Featherstone RM (1961) A new and rapid colorimetric determination of acetylcholinesterase activity. Biochem Pharmacol 7:88–95
Emre Kızıl H, Gür C, Ayna A, Darendelioğlu E, Küçükler S, Sağ S (2023) Contribution of oxidative stress, apoptosis, endoplasmic reticulum stress and autophagy pathways to the ameliorative effects of hesperidin in NaF-induced testicular toxicity. Chem Biodivers 20:e202200982
Fereidouni S, Kumar RR, Chadha VD, Dhawan DK (2019) Quercetin plays protective role in oxidative induced apoptotic events during chronic chlorpyrifos exposure to rats. J Biochem Mol Toxicol 33:e22341
Ghahremani S, Soodi M, Atashi A (2018) Quercetin ameliorates chlorpyrifos-induced oxidative stress in the rat brain: possible involvment of PON2 pathway. J Food Biochem 42:e12530
Hassan AA, Bel Hadj Salah K, Fahmy EM, Mansour DA, Mohamed SAM, Abdallah AA et al (2022) Olive leaf extract attenuates chlorpyrifos-induced neuro- and reproductive toxicity in male albino rats. Life 12,
Hsu S-S, Lin Y-S, Chen H-C, Liang W-Z (2023) Involvement of oxidative stress-related apoptosis in chlorpyrifos-induced cytotoxicity and the ameliorating potential of the antioxidant vitamin E in human glioblastoma cells. Environ Toxicol 38:2143–2154
Kandemir FM, Ozkaraca M, Küçükler S, Caglayan C, Hanedan B (2018) Preventive effects of hesperidin on diabetic nephropathy induced by streptozotocin via modulating TGF-β1 and oxidative DNA damage. Toxin Reviews 37:287–293
Kaur S, Singla N, Dhawan DK (2019) Neuro-protective potential of quercetin during chlorpyrifos induced neurotoxicity in rats. Drug Chem Toxicol 42:220–230
Khalaf AA, Ogaly HA, Ibrahim MA, Abdallah AA, Zaki AR, Tohamy AF (2022) The reproductive injury and oxidative testicular toxicity induced by chlorpyrifos can be restored by zinc in male rats. Biol Trace Elem Res 200:551–559
Kızıl HE, Caglayan C, Darendelioğlu E, Ayna A, Gür C, Kandemir FM et al (2023) Morin ameliorates methotrexate-induced hepatotoxicity via targeting Nrf2/HO-1 and Bax/Bcl2/Caspase-3 signaling pathways. Mol Biol Rep 50:3479–3488
Koksal Z, Kalin R, Gulcin I, Ozdemir H (2018) Inhibitory effects of selected pesticides on peroxidases purified by affinity chromatography. Int J Food Prop 21:385–394
Küçükler S, Çomaklı S, Özdemir S, Çağlayan C, Kandemir FM (2021) Hesperidin protects against the chlorpyrifos-induced chronic hepato-renal toxicity in rats associated with oxidative stress, inflammation, apoptosis, autophagy, and up-regulation of PARP-1/VEGF. Environ Toxicol 36:1600–1617
Landis WG, Chu VR, Graham SE, Harris MJ, Markiewicz AJ, Mitchell CJ et al (2020) Integration of chlorpyrifos acetylcholinesterase inhibition, water temperature, and dissolved oxygen concentration into a regional scale multiple stressor risk assessment estimating risk to Chinook salmon. Integr Environ Assess Manag 16:28–42
Lawrence RA, Burk RF (1976) Glutathione peroxidase activity in selenium-deficient rat liver. Biochem Biophys Res Commun 71:952–958
Lionetto MG, Caricato R, Giordano ME (2020) Carbonic anhydrase sensitivity to pesticides: perspectives for biomarker development. Int J Mol Sci 21,
Livak KJ, Schmittgen TD (2001) Analysis of relative gene expression data using real-time quantitative PCR and the 2− ΔΔCT method. Methods 25:402–408
Lowry OH, Rosebrough NJ, Farr AL, Randall RJ (1951) Protein measurement with the Folin phenol reagent. J Biol Chem 193:265–275
Mahmoud SM, Abdel Moneim AE, Qayed MM, El-Yamany NA (2019) Potential role of N-acetylcysteine on chlorpyrifos-induced neurotoxicity in rats. Environ Sci Pollut Res 26:20731–20741
Nandhini AR, Harshiny M, Gummadi SN (2021) Chlorpyrifos in environment and food: a critical review of detection methods and degradation pathways. Environ Science: Processes Impacts 23:1255–1277
Obeng E (2020) Apoptosis (programmed cell death) and its signals-A review. Brazilian J Biology 81:1133–1143
Owumi SE, Najophe ES, Otunla MT (2022) 3-Indolepropionic acid prevented chlorpyrifos-induced hepatorenal toxicities in rats by improving anti-inflammatory, antioxidant, and pro-apoptotic responses and abating DNA damage. Environ Sci Pollut Res 29:74377–74393
Ozturk Kurt B, Ozdemir S (2023) Selenium heals the chlorpyrifos-induced oxidative damage and antioxidant enzyme levels in the rat tissues. Biol Trace Elem Res 201:1772–1780
Placer ZA, Cushman LL, Johnson BC (1966) Estimation of product of lipid peroxidation (malonyl dialdehyde) in biochemical systems. Anal Biochem 16:359–364
Samina S (2017) Oxidative stress and the central nervous system. J Pharmacol Exp Ther 360:201
Sedlak J, Lindsay RH (1968) Estimation of total, protein-bound, and nonprotein sulfhydryl groups in tissue with Ellman's reagent. Anal Biochem 25:192–205
Seth E, Ahsan AU, Kaushal S, Mehra S, Chopra M (2021) Berberine affords protection against oxidative stress and apoptotic damage in F1 generation of Wistar rats following lactational exposure to chlorpyrifos. Pestic Biochem Physiol 179:104977
Singh V, Panwar R (2014) In vivo antioxidative and neuroprotective effect of 4-Allyl-2-methoxyphenol against chlorpyrifos-induced neurotoxicity in rat brain. Mol Cell Biochem 388:61–74
Sulumer AN, Palabıyık E, Avcı B, Uguz H, Demir Y, Serhat Özaslan M et al (2023) Protective effect of bromelain on some metabolic enzyme activities in tyloxapol-induced hyperlipidemic rats. Biotechnol Appl Chem ; n/a.
Sun Y, Oberley LW, Li Y (1988) A simple method for clinical assay of superoxide dismutase. Clin Chem 34:497–500
Topal A, Atamanalp M, Oruç E, Demir Y, Beydemir Ş, Işık A (2014) In vivo changes in carbonic anhydrase activity and histopathology of gill and liver tissues after acute exposure to chlorpyrifos in rainbow trout. Archives of Industrial Hygiene and Toxicology 65:377–385
Uzun FG, Kalender Y (2013) Chlorpyrifos induced hepatotoxic and hematologic changes in rats: the role of quercetin and catechin. Food Chem Toxicol 55:549–556
Varışlı B, Darendelioğlu E, Caglayan C, Kandemir FM, Ayna A, Genç A et al (2022) Hesperidin attenuates oxidative stress, inflammation, apoptosis, and cardiac dysfunction in sodium fluoride-induced cardiotoxicity in rats. Cardiovasc Toxicol 22:727–735
Verpoorte JA, Mehta S, Edsall JT (1967) Esterase activities of human carbonic anhydrases B and C. J Biol Chem 242:4221–4229
Wang T, Zheng L, Zhang W (2021) Hesperidin alleviates bupivacaine anesthesia-induced neurotoxicity in SH-SY5Y cells by regulating apoptosis and oxidative damage. J Biochem Mol Toxicol 35:e22787
Wardyn Joanna D, Ponsford Amy H, Sanderson Christopher M (2015) Dissecting molecular cross-talk between Nrf2 and NF-κB response pathways. Biochem Soc Trans 43:621–626
Wdowiak K, Walkowiak J, Pietrzak R, Bazan-Woźniak A, Cielecka-Piontek J. (2022) Bioavailability of hesperidin and its aglycone

hesperetin—compounds found in citrus fruits as a parameter conditioning the pro-health potential (neuroprotective and anti-diabetic activity)—Mini-Review. Nutrients. 14.

Yazdinezhad A, Abbasian M, Hojjat Hosseini S, Naserzadeh P, Agh-Atabay A-H, Hosseini M-J (2017) Protective effects of Ziziphora tenuior extract against chlorpyrifos induced liver and lung toxicity in rat: mechanistic approaches in subchronic study. Environ Toxicol 32:2191–2202

Zhang Y, Chang Y, Cao H, Xu W, Li Z, Tao L (2018) Potential threat of chlorpyrifos to human liver cells via the caspase-dependent mitochondrial pathways. Food Agr Immunol 29:294–305